Novel Control Strategy for a UPQC under Distorted Source and Nonlinear Load Conditions

Quoc-Nam Trinh[*] and Hong-Hee Lee[†]

[*†]School of Electrical Engineering, University of Ulsan, Ulsan, Korea

Abstract

This paper proposes a novel control strategy for a unified power quality conditioner (UPQC) including a series and a shunt active power filter (APF) to compensate the harmonics in both the distorted supply voltage and the nonlinear load current. In the series APF control scheme, a proportional-integral (PI) controller and a resonant controller tuned at six multiples of the fundamental frequency of the network ($6\omega_S$) are performed to compensate the harmonics in the distorted source. Meanwhile, a PI controller and three resonant controllers tuned at $6n\omega_S$ (n=1, 2, 3) are designed in the shunt APF control scheme to mitigate the harmonic currents produced by nonlinear loads. The performance of the proposed UPQC is significantly improved when compared to that of the conventional control strategy thanks to the effective design of the resonant controllers. The feasibility of the proposed UPQC control scheme is validated through simulation and experimental results.

Key words: Active Power Filter (APF), Harmonic compensation, Resonant controller, Unified Power Quality Conditioner (UPQC)

I. INTRODUCTION

Power quality problems have been increasingly causing concerns due to the wide use of nonlinear loads such as adjustable speed drives, electric arc welders, and the switching power supplies in distribution systems. Nonlinear loads cause harmonic currents in networks and consequently distort the voltage waveform at the point of common coupling (PCC) due to system impedances. This distorted voltage waveform harmfully affects the other loads connected at the PCC. To avoid this problem and to protect loads from distortions, the harmonic components of the voltage and current must be fully compensated.

LC passive filters and shunt active power filters (APFs) are regularly used to mitigate harmonic currents [1], [2]. However, this method does not have a control effort to reduce the voltage harmonics at the PCC since it is only capable of dealing with harmonic current problems. In other words, even though harmonic currents are successfully compensated, the voltage waveform at the PCC is unable to be sinusoidal.

In order to simultaneously deal with harmonic voltage and current problems, an advanced solution, i.e., the unified

power quality conditioner (UPQC) has been developed [2], [3]. The UPQC is composed of a shunt and a series APF to ensure that both the load voltage and the supply current become sinusoidal, where the shunt APF is operated as a controlled current source to compensate the harmonic currents produced by nonlinear loads. Meanwhile, the series APF acts as a controlled voltage source to compensate the harmonics of the supply voltage. Various UPQC control schemes have been developed to mitigate harmonic voltages and currents [2]-[14]. The majority of the previous studies are based on the *p-q* theory and they require too many sensors: three sets of current sensors and two sets of voltage sensors, as shown in Fig. 1 [2]-[5].

In Fig. 1, in order to compensate the distorted voltage and current, the harmonic components in the supply voltage and in the load current are detected through harmonic detectors and regulated by hysteresis controllers. The harmonic detectors are regularly realized by using a low-pass filter (LPF) or a high-pass filter (HPF) in the fundamental reference (*d-q*) frame [13]. The harmonic detectors should be designed carefully to achieve both a fast dynamic response and good steady-state performance for the UPQC. Otherwise, the whole control performance of the UPQC may be deteriorated. Even though hysteresis controllers are robust and easy to implement, they still suffer from two main shortcomings. First, the output filters of the converters are difficult to design, due to the varying switching frequency.
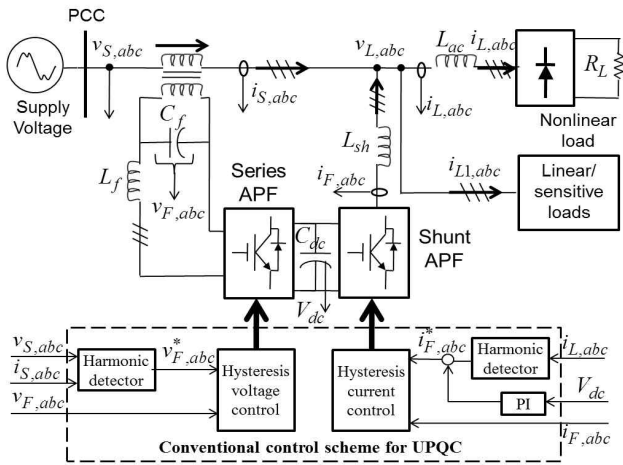
Fig. 1. Block diagram of the conventional UPQC control scheme.

Second, the control performance is limited by a trade-off between the hysteresis band (HB) and the switching frequency. If the HB is designed to be small, the control performance may be better. On the other hand, if the switching frequency becomes high, the switching loss is increased.

Recently, indirect control techniques have been introduced to simplify the control scheme, where the load voltage and the supply current are measured and regulated instead of the filter voltage and current [6]-[14]. As a result, the harmonic detectors are eliminated and the number of sensors is reduced. Only two sets of voltage sensors and one set of current sensors are needed to implement the UPQC. However, since these control strategies are still developed by using hysteresis controllers, good control performance cannot be achieved since switching ripples appear in the load voltage and in the supply current.

To improve the performance of a UPQC, this paper proposes a novel control strategy with the aid of proportional-integral (PI) and resonant controllers. In the series APF control scheme, a PI controller plus a resonant controller tuned at six multiples of the fundamental frequency of the network ($6\omega_S$) are used to compensate harmonic voltages. Meanwhile in the shunt APF control scheme, a PI controller and three resonant controllers tuned at $6n\omega_S$ (n=1, 2, 3) are used to mitigate harmonic currents. As a result, the load voltage and the supply current can be regulated to be sinusoidal waveforms. Owing to the effective design of the resonant controllers, the control performance of the UPQC is significantly improved when compared to conventional control strategies. The feasibility of the proposed UPQC control scheme is verified through simulation and experimental results.

II. PROPOSED UPQC CONTROL STRATEGY

Fig. 2 shows a block diagram of the proposed UPQC control scheme. As shown in Fig. 2, the proposed control scheme does not require harmonic detectors. The load voltage and the supply current are directly measured and regulated to be sinusoidal by the proposed PI-R voltage controller and the PI-3R current controller. Due to the absence of harmonic detection in the proposed control strategy, the accuracy and the steady-state performance of the UPQC can be significantly improved.

A. Proposed PI-R Voltage Controller

The main objective of the series APF is to compensate the harmonic voltages in a distorted source to keep the load voltage sinusoidal.

Assuming that the source voltage, available at the PCC (v_S), is distorted and includes fundamental (v_{S1}) and harmonic components (v_{Sh}), as defined in (1):

$$v_S(\omega t) = v_{S1} + \sum_{h \neq 1} v_{Sh} . \tag{1}$$

To make the load voltage sinusoidal, the harmonic components presented in (1) must be completely compensated. In three-phase systems, the harmonic voltages have odd components ($6n\pm1$, where n = 1, 2, 3...) of the fundamental frequency of the network (ω_S). Among these harmonics, the fifth and seventh harmonics are the most severe components that need to be eliminated.

A resonant controller is an effective solution to regulate specific ac signals [15]. Two resonant controllers tuned at $5\omega_S$ and $7\omega_S$ are able to sufficiently track the fifth and seventh harmonics. Moreover, since both the fifth and seventh harmonics become the sixth harmonic in the d-q frame, one resonant controller with a resonant frequency of $6\omega_S$ is also capable of simultaneously compensating both the fifth and seventh harmonic voltages. As a result, the control scheme is simplified since only one controller is needed to regulate two harmonics. The open-loop transfer function of the resonant
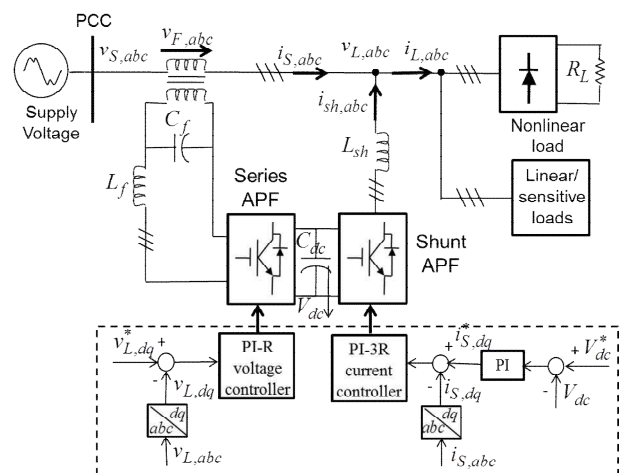

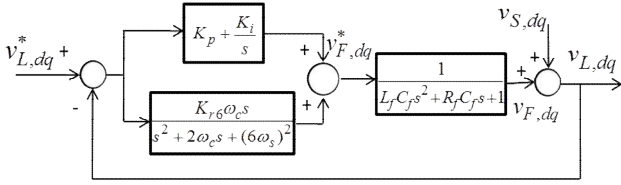Fig. 2. Block diagram of the proposed UPQC control scheme.

Fig. 3. Proposed PI-R voltage controller.

controller is defined as (2).

$$G_R = \frac{K_{r6}\omega_c s}{s^2 + 2\omega_c s + (6\omega_s)^2} \qquad (2)$$

where K_{r6} and ω_c are the resonant gain and the cut-off frequency of the resonant controller, respectively.

In addition, a PI controller is utilized to compensate a small voltage drop resulting from the system impedance and the series transformer. It is also used to improve the dynamic response of the series APF. Consequently, the voltage control scheme for the series APF consists of a PI controller and a resonant controller, and the combined transfer function is given as follows:

$$G_{PI-R} = K_p + \frac{K_i}{s} + \frac{K_{r6}\omega_c s}{s^2 + 2\omega_c s + (6\omega_s)^2} \qquad (3)$$

where K_p and K_i are the proportional and integral gain of the PI controller, respectively.

A block diagram of the proposed voltage controller for the series APF is illustrated in Fig. 3.

B. Proposed PI-3R Current Controller

The purpose of a shunt APF is to mitigate the harmonic currents produced by nonlinear loads. The nonlinear load under consideration is a three-phase diode rectifier supplying a dc load. This type of load induces harmonic currents into the networks, which have odd orders ($6n\pm1$, where $n = 1, 2, 3...$) of ω_s. To make the supply current sinusoidal, a shunt APF must inject harmonic currents with the same magnitudes and opposite phases as those in the nonlinear load current. In addition, the shunt APF has a responsibility to maintain the common DC-link voltage of series and shunt APFs (V_{dc}) in a stable manner. As a result, the shunt APF control scheme includes an outer voltage control loop and an inner current control loop, as shown in Fig. 2.

In the V_{dc} voltage control loop, a simple PI controller is sufficient to regulate the DC-link voltage to be constant with a desired value because the DC-link voltage has a slow dynamic response. However, in the current control loop, since the shunt APF must generate harmonic currents which are high frequency signals, the PI controller is no longer adequate to regulate the harmonic currents. As a result, a resonant controller is utilized instead of a PI controller.
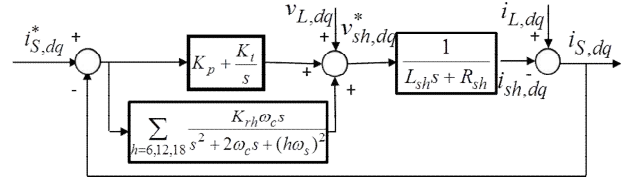

Fig. 4. Proposed PI-3R current controller.

It is the same as the harmonics in the voltage case where the ($6n\pm1$) harmonic currents become $6n$ harmonics in the d-q frame. Hence one resonant controller with a resonant frequency of $6n\omega_s$ is capable of regulating a pair of ($6n\pm1$) harmonic currents. Therefore, the number of controllers is reduced by half. In fact, the effects of very high order harmonics can be negligible. In this paper, only the first six (up to 19th) harmonics are considered to be compensated. Accordingly, three resonant controllers are needed to regulate these six harmonic currents. The open-loop transfer function of the resonant controller is described as follows:

$$G_{3R} = \sum_{h=6,12,18} \frac{K_{rh}\omega_c s}{s^2 + 2\omega_c s + (h\omega_s)^2} \qquad (4)$$

where h=6, 12, 18 are the orders of the harmonic currents in the d-q frame.

In addition, a PI controller is also needed to regulate the fundamental current to charge the DC-link capacitor. As a result, the current controller of the shunt APF consists of a PI controller and three resonant controllers, as shown in Fig. 4.

C. Improved Phase-Locked Loop Scheme

The purpose of the PLL is to detect the phase angle of the supply voltage for grid synchronization, which is an essential part of power converters for interfacing with the grid. In addition, since the proposed control algorithm is designed in the d-q frame, the phase angle of the supply voltage is necessary for coordinate transformation. However, a conventional PLL is unable to operate properly under distorted supply voltage conditions. Hence a low-pass filter (LPF) is added before the PLL block, as shown in Fig. 5, to reject the effects of harmonic voltages on the PLL performance. In Fig. 5, the LPF is used in the d-q frame. Therefore, there is no time delay problem due to the LPF which can affect the PLL accuracy and the UPQC performance because the fundamental component becomes a DC signal in the d-q frame.

In practical applications, if the phase angle of the supply voltage is not detected correctly due to a time delay of the PLL, the system can be seriously damaged at the connecting time of the UPQC due to a spike or an overshoot of the supply current. In addition, the coordinate transformation cannot be performed correctly. As a result, the UPQC control performance is deteriorated.
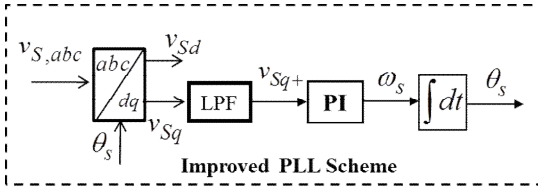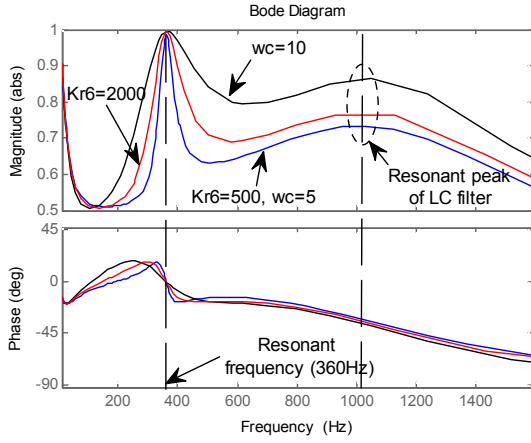
Fig. 5. Block diagram of the improved PLL scheme.

Fig. 6. Bode diagram of closed-loop transfer function of proposed voltage controller.

III. ANALYSIS AND DESIGN OF THE VOLTAGE AND CURRENT CONTROLLERS

A. Analysis and Design of the Proposed Voltage Controller

To assess the performance of the proposed voltage controller in compensating the fifth and seventh harmonic voltages, the closed-loop transfer function of the proposed voltage controller, which is described by (5), is analyzed.

$$G_C = \frac{G_{PI-R}(s)G_{LC}(s)}{1+G_{PI-R}(s)G_{LC}(s)} \quad (5)$$

where $G_{LC} = 1/(L_f C_f s^2 + R_f C_f s + 1)$ is the transfer function of the LC filter.

The Bode diagram of (5) with respect to different values of K_{r6} and ω_c is shown in Fig. 6. It can be seen that the voltage controller provides a unity gain and zero phase-shift at the selected resonant frequency, i.e., six multiple of the fundamental frequency (360Hz) regardless of the values of K_{r6} and ω_c. This means that the proposed voltage controller is capable of tracking the sixth harmonics with zero steady-state error. As mentioned before, the fifth and seventh harmonics become the sixth harmonic in the d-q frame. Hence, if the proposed controller can regulate the sixth harmonic with zero steady-state error, the fifth and seventh harmonics will be mitigated too.

Although the proposed PI-R controller theoretically

provides zero steady-state error at the selected resonant frequency regardless of the controller gains, the controller gains must be designed carefully based on the plant (LC filter) parameters to guarantee system stability. In this paper, the Naslin polynomial technique, which is general and applicable to many control system [16], [17], is used to determine the controller gains. According to [16], the controller gains are computed based on the fourth-order Naslin polynomial given as:

$$N(s) = a_0\left(1+\frac{s}{\omega_n}+\frac{s^2}{\alpha\omega_n^2}+\frac{s^3}{\alpha^3\omega_n^3}+\frac{s^4}{\alpha^6\omega_n^4}\right) \quad (6)$$

where α is the characteristic ratio, a_0 is the coefficient, and ω_n is the Naslin frequency.

By matching the coefficients in (6) with those in the nominator of the closed-loop transfer function in (5), the controller gains are determined as follows:

$$K_p = \frac{(6\omega_s)^2}{\alpha^3\omega_n^3} - L_f C_f (6\omega_s)^2 - 1$$

$$K_i = \left(\frac{(6\omega_s)^2}{\alpha^3\omega_n^3} - L_f C_f (6\omega_s)^2\right)\omega_n$$

$$K_{r6} = \frac{(6\omega_s)^2}{\alpha\omega_n^2} - R_f C_f (6\omega_s)^2 \quad (7)$$

$$\omega_n = \frac{6\omega_s}{R_f}\sqrt{\frac{L_f}{C_f}}$$

where the characteristic ratio of the Naslin polynomial is selected as $\alpha = 2$.

Generally, a small cut-off frequency, ω_c, within the range of 5-15 rad/s can be selected in practical implementation [18]. In this paper, a cut-off frequency, ω_c, of 10 rad/s is chosen to achieve good steady-state performance and an adequately fast dynamic response.

B. Analysis and Design of the Proposed Current Controller

In order to determine whether the proposed current controller sufficiently regulates harmonic currents, the closed-loop transfer function of the proposed current controller in (8) is analyzed.

$$G_C = \frac{G_{PI-3R}(s)G_L(s)}{1+G_{PI-3R}(s)G_L(s)} \quad (8)$$

where $G_L = 1/(L_{sh}s + R_{sh})$ is the transfer function of the L_{sh} inductor.

The Bode diagram of (8) with respect to different values of K_{rh} and ω_c is plotted in Fig. 7. Fig. 7 shows that the resonant controller provides a unity gain (0 dB) and zero phase-shift at selected resonant frequencies, i.e., 360Hz, 720Hz, and 1080Hz, regardless of the value of K_{rh} and ω_c.
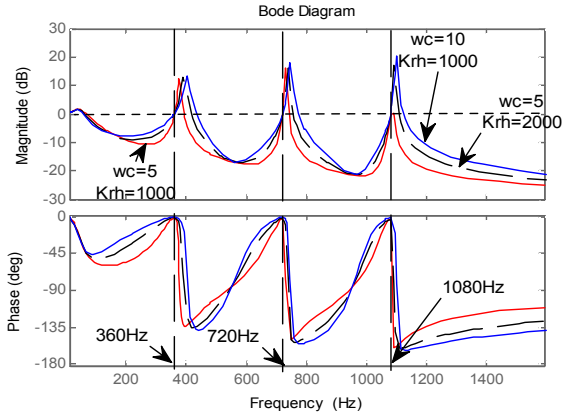
Fig. 7. Bode diagram of closed-loop transfer function of proposed current controller.

This shows that the proposed current controller is able to regulate the selected harmonic currents with zero steady-state error.

The Naslin polynomial technique is also used to design the controller gains of the current controller. In fact, since the current controller has three resonant controllers, a higher order of the Naslin polynomial should be used to determine all of the controller gains. However, this makes the design process very complicated. To avoid this problem, only the PI controller and one resonant controller tuned at the sixth harmonic are taken into account, and the other resonant gains are determined based on K_{r6}. Using the fourth-order Naslin polynomial given in (6), the controller gains are computed as follows:

$$K_p = L_{sh}\frac{\omega_n}{\alpha^3} - R_{sh}$$

$$K_i = L_{sh}\frac{\omega_n^2}{\alpha^3}$$

$$K_{r6} = L_{sh}\frac{\omega_n^2}{\alpha}\left(\alpha + 1 - \frac{1}{\alpha^2}\right) \tag{9}$$

$$\omega_n = \frac{6\omega_s}{\sqrt{\alpha^3}}$$

where the characteristic ratio of the Naslin polynomial is selected as $\alpha = 2$.

IV. SIMULATION RESULTS

The simulation model consists of a UPQC and a nonlinear load supplied by a distorted source where the total harmonic distortion (THD) factors of the non-linear load and the distorted source are 25.2% and 16.5%, respectively. The detail system parameters are given in Table I. The simulations are performed by using PSIM software.

TABLE I
SYSTEM PARAMETERS

|	**Parameters**		**Value**
Supply	Fundamental voltage	$V_{S,abc}$	110 V_{rms}
	Frequency	f_S	60 Hz
	Fifth order voltage		15%
	Seventh order voltage		7%
Load	3-phase AC inductance	L_{ac}	2 mH
	Diode rectifier load resistance	R_L	20 Ω
DC-link	Reference voltage	V_{dc}^*	350 V
	Capacitance	C_{dc}	2.2 mF
Shunt APF	Filter inductance	L_{sh}	3.5 mH
	Switching frequency	f_{sw}	5 kHz
Series APF	Filter inductance	L_f	0.7 mH
	Filter capacitance	C_f	27 μF
	Switching frequency	f_{sw}	5 kHz
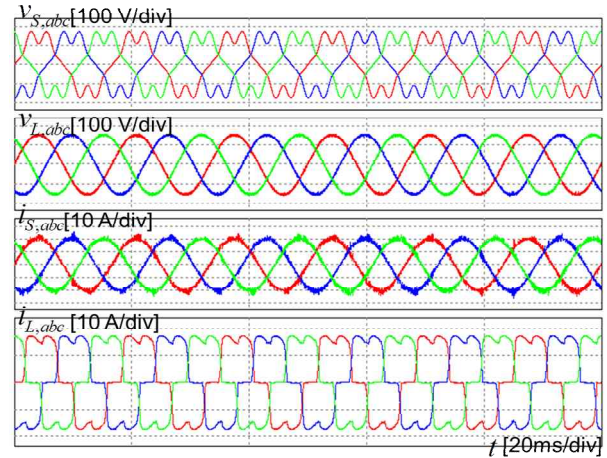
Fig. 8. Simulation results with the conventional control scheme.

First, the conventional control scheme reported in [10], where hysteresis controllers are used, is simulated. In this simulation, the HBs of the voltage and current controllers are selected as 2% and 3% of their reference values, respectively. The results are shown in Fig. 8. As depicted in Fig. 8, even though a small HB is used, the performance of the load voltage and the supply current are not good, since there are some distortions in those waveforms. These distortions are caused by switching frequency variations of the hysteresis controller. The switching frequency varies over a wide range and the output filter is unable to cancel all of the switching noises. In this case, ripples in the load voltage and the supply current influence each other. Ripples in the supply current make the load voltage more distorted due to the system and series transformer impedance. In turn, this distorted voltage waveform affects the performance of the shunt APF. As a result, the high frequency distortions are left with a high THD factor in the load voltage
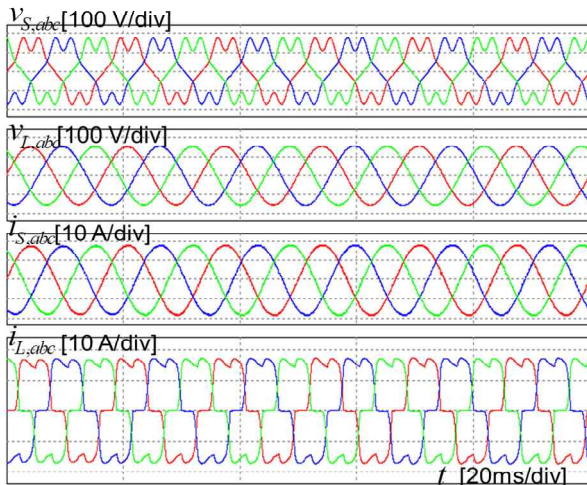
Fig. 9. Simulation results with the proposed control scheme.

Fig. 10. Dynamic response of UPQC with the proposed control scheme.

Fig. 11. Dynamic response of UPQC with the conventional control scheme.

and supply current, which are 3.9% and 7.4%, respectively. These results do not comply with the IEEE-519 harmonic standards [19]. Moreover, due to the small HB's, the switching frequency is very high, which results in a higher power loss in the UPQC.

To demonstrate the superiority of the proposed control algorithm, the proposed control scheme is also simulated under the same conditions as those used in Fig. 8. The results are presented in Fig. 9. Fig. 9 reveals that the harmonics in the supply voltage and the nonlinear load current are effectively compensated, and that the load voltage and the supply current become almost sinusoidal waveforms with small THD factors of approximately 1.2% and 1.95%, respectively. This completely meets the IEEE 519 standards. In Fig. 9, the load voltage and the supply current do not contain switching noises since the switching frequency of the proposed algorithm is fixed. In addition, since the switching frequency of the proposed method is relatively lower (5 kHz) when compared to that of the hysteresis controller (18 kHz average), the power loss is significantly reduced. From these comparative results, the effectiveness of the proposed control scheme is verified.

Along with good steady-state performance, a fast dynamic response is also an important factor in UPQC performance because the load voltage and the supply current should be compensated to be sinusoidal as soon as possible during load variations. To evaluate the dynamic performance of the proposed control strategy, the transient responses of the UPQC are illustrated in Fig. 10. Fig. 10 shows that when the UPQC is activated at a 50% load, it takes less than one fundamental cycle for the UPQC to completely compensate harmonics in the supply voltage and in the nonlinear load current to make the load voltage and the supply current sinusoidal. After that, when the load is changed from 50% to 100%, the UPQC also responds quickly to load changes to mitigate harmonics in the load current and to guarantee that
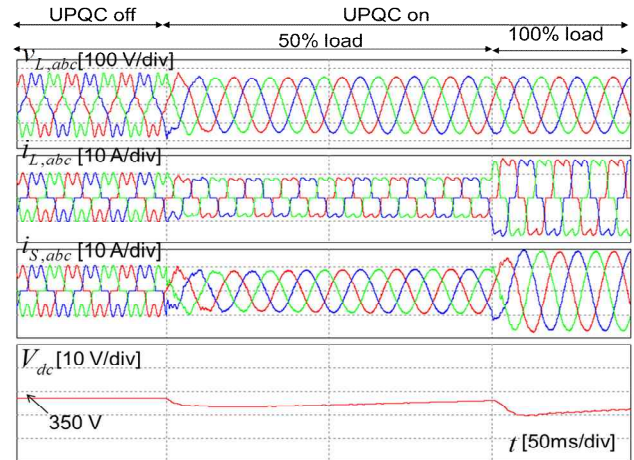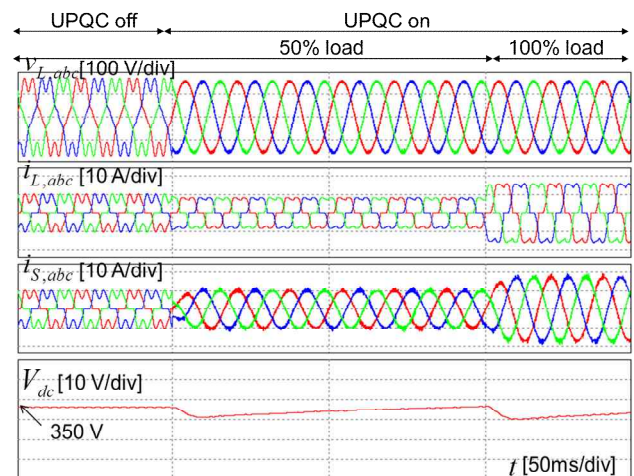
both the load voltage and supply current always become sinusoidal. It is noticed that the supply current also needs around one cycle to settle at the steady-state value. Actually, due to limitation on the control bandwidth of the DC-link voltage control loop, a one cycle response time for the supply current is enough. Moreover, this result is much better than the results reported in [10] and [11] where the dynamic response of the supply current is more than two cycles.

Fig. 11 presents the dynamic responses of a UPQC with a hysteresis controller. As shown in Fig. 11, thanks to the fast response characteristic of the hysteresis controller, the load voltage is immediately compensated to be sinusoidal when the UPQC is operated. However, the supply current takes about one cycle to settle at its steady-state, which is similar to the results shown in Fig. 10. This is due to the fact that the dynamic response of the supply current depends on not only the hysteresis controller but also on the DC-link voltage controller. As a result, the dynamic response of the UPQC with a hysteresis controller is similar to that obtained with the

	Proposed control scheme	Conventional control scheme [10]
THD values	1.2% (Load voltage) 1.95%(Supply current)	3.9% (Load voltage) 7.4%(Supply current)
Switching frequency	Fixed (5 kHz)	Variable (18 kHz average)
Dynamic response	Less than one fundamental cycle	More than two fundamental cycles
Power loss	352W (13kVA load)	687W (13kVA load)

proposed control scheme. However, it is obvious that steady-state performance is worse than that of the proposed control scheme.

Table II shows a summary of the comparison between the proposed control algorithm and the conventional one in [10]. As presented in Table II, by using the proposed control scheme, the THD values of the load voltage and the supply current are significantly reduced when compared with those of the conventional control method. In addition, the proposed control scheme provides a much faster dynamic response. Moreover, the power loss of the conventional control scheme is intensively increased because a small HB is used to achieve acceptable performance.

V.   EXPERIMENTAL RESULTS

An overview of the experimental system is shown in Fig. 12. All of the parameters in the experimental system are the same as those used in the simulation model given in Table I. The control strategy is implemented using a floating-point DSP (TMS320F28335 of Texas Instruments). The control and switching frequencies are set at 10 kHz and 5 kHz, respectively. The distorted supply voltage is generated by a Programmable AC Power Source (Chroma 61704).

Fig. 13 shows the experimental results of the proposed control strategy, where the supply voltage, the load voltage, the FFT of the load voltage, the supply current, the FFT of the supply current, and the load current are plotted from the top to the bottom, respectively. In Fig. 13, even though the supply voltage and the load current are highly distorted, both the load voltage and the supply current are effectively compensated to be sinusoidal thanks to the effectiveness of the proposed control algorithm. The THD values of the load voltage and the supply current in the experiment are 1.55% and 2.14%, respectively. In fact, the THD values in the experiment are slightly higher than those in the simulation due to the measurement and switching noises that are inevitable in experiments. However, these THD values still satisfy the IEEE-519 standards.

The dynamic responses of the system before and after the UPQC is activated are shown in Fig. 14. The load voltage and
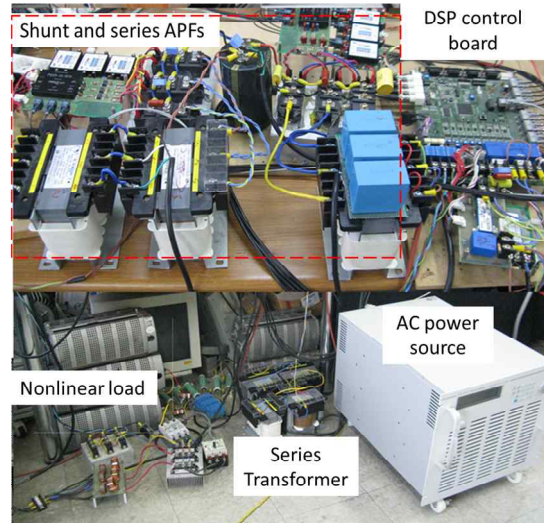

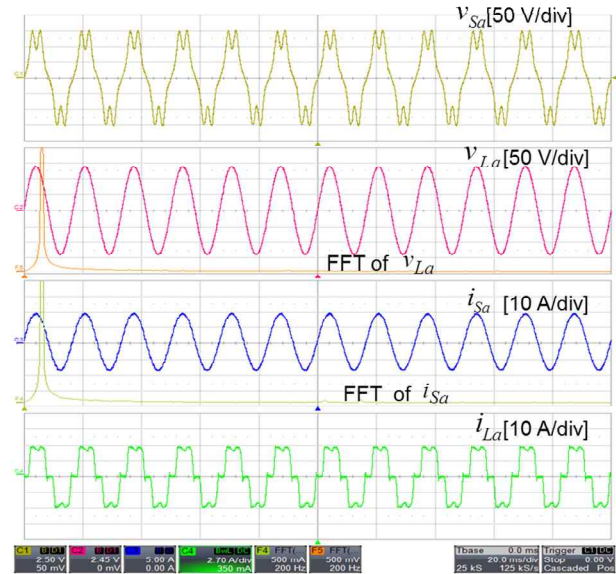Fig. 12. Experimental platform for the UPQC.

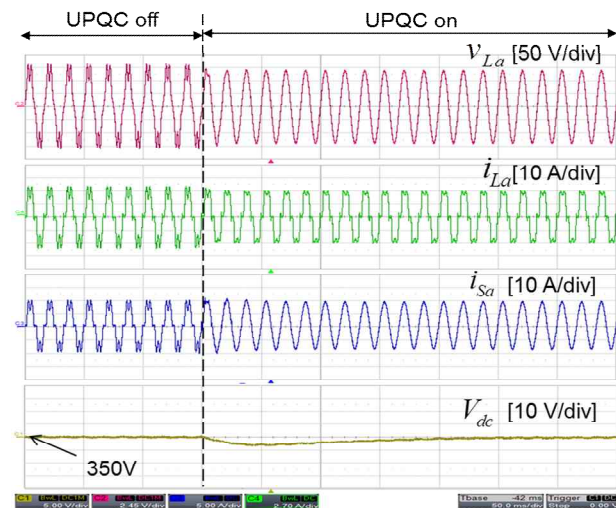Fig. 13. Steady-state performance of the proposed control scheme.

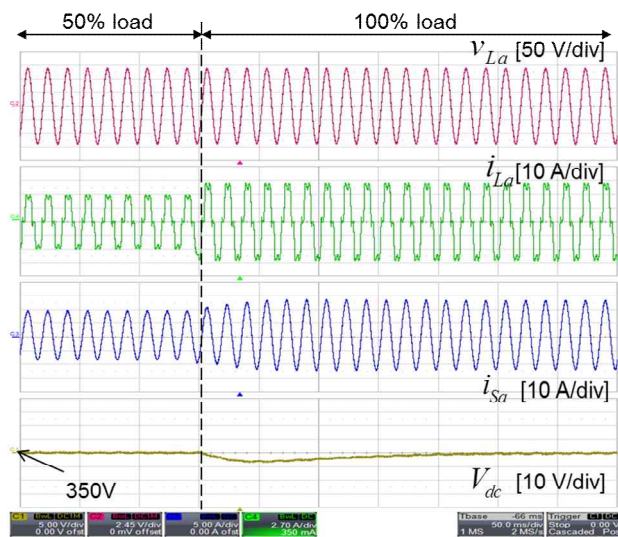Fig. 14. Dynamic response when UPQC is activated.

Fig. 15. Dynamic response of UPQC when load change.

the supply current are highly distorted before the UPQC is activated. However, as soon as the UPQC starts to operate, the load voltage and the supply current are compensated to be sinusoidal without experiencing any oscillation or overshoot during the transient time.

Fig. 15 illustrates dynamic responses of the UPQC when load is changed from 50% to 100% of its rated value. It is obvious that the UPQC quickly responds to the change to mitigate the harmonics in the load current and to make both the load voltage and the supply current sinusoidal. As in the simulation results, it takes less than one fundamental cycle for the supply current to settle at its steady-state value.

Finally, it can be said that the experimental results coincide with those of the simulation, and that the proposed control scheme has good performance.

VI. CONCLUSIONS

In this paper, a novel control strategy for a UPQC was proposed with the aid of PI and resonant controllers. The proposed control strategy was investigated and the design of the PI and resonant controllers were also presented in detail. Only one resonant controller gain was designed for simplicity. The other gains were determined by using the relationship between the resonant frequency and the controller gain. Despite a simple design process, the proposed control strategy provides good steady-state performance as well as fast dynamic responses against load variations. The load voltage and the supply current are effectively compensated to be sinusoidal. In both the simulations and experiments, the THD values of the load voltage and the supply current are reduced to comply with the IEEE-519 standards.

In this paper, a UPQC under distorted source and nonlinear load conditions has been considered by assuming that they are all balanced in order to show the effectiveness of the proposed controller. However, the supply voltage and the load current can be also unbalanced, and this will be investigated in a future study on the basis of the proposed control principle.

REFERENCES

[1]   H. Akagi, "New trends in active filters for power conditioning," *IEEE Trans. Ind. Applicat.*, Vol. 32, pp. 1312-1332, Nov./Dec. 1996.

[2]   H. Akagi, E. H. Watanabe, and M. Aredes, *Instantaneous Power Theory and Applications to Power Conditioning*. Hoboken, NJ: Wiley-IEEE Press, Apr. 2007.

[3]   H. Fujita and H. Akagi, "The unified power quality conditioner: The integration of series and shunt active filters," *IEEE Trans. Power Electron.*, Vol. 13, No. 2, pp. 315-322, Mar. 1998.

[4]   D. Graovac, V. Katic, and A. Rufer, "Power quality problems compensation with universal power quality conditioning system," *IEEE Trans. Power Del.,* Vol. 22, No. 2, pp. 968-976, Apr. 2007.

[5]   B. Han, B. Bae, H. Kim, and S. Baek, "Combined operation of unified power quality conditioner with distributed generation," *IEEE Trans. Power Del.,* Vol. 21, No. 1, pp. 330-338, Jan. 2006.

[6]   E. Ozdemir, M. Ucar, M. Kesler, and M. Kale, "A simplified control algorithm for shunt active power filter without load and filter current measurement," in *Proc. 32nd IEEE IECON*, pp. 2599-2604, 2006.

[7]   Y. Pal, A. Swarup, and B. Singh, "Control strategy for selective compensation of power quality problems through three-phase four-wire upqc," *Journal of Power Electronics*, Vol. 11, No. 4, pp. 576-582, Jul. 2011.

[8]   B. Singh and Venkateswarlu P, "A simplified control algorithm for three-phase, four-wire unified power quality conditioner," *Journal of Power Electronics*, Vol. 10, No. 1, pp. 91-96, Jan. 2010.

[9]   I. Axente, M. Basu, M. F. Conlon, and K. Gaughan, "A 12-kVA dsp-controlled laboratory prototype upqc capable of mitigating unbalance in source voltage and load current," *IEEE Trans. Power Del.*, Vol. 25, No. 6, pp. 1302-1309, Jun. 2010.

[10] M. Kesler and E. Ozdemir, "Synchronous reference frame based control method for upqc under unbalanced and distorted load conditions," *IEEE Trans. Ind. Electron.*, Vol. 58, No. 9, pp. 3967-3975, Sep. 2011.

[11] V. Khadkikar, A. Chandra, A. O. Barry, and T. D. Nguyen, "Power quality enhancement utilizing single phase unified power quality conditioner: digital signal processor-based experimental validation," *IET Power Electronics*, Vol. 4, No. 3, pp. 323-331, Mar. 2011.

[12] V. Khadkikar and A. Chandra, "A novel structure for three, "phase four-wire distribution system   utilizing unified power quality conditioner (upqc)," *IEEE Trans. Ind. Appl.*, Vol. 45, No.5, pp. 1897-1902, Sep./Oct. 2009.

[13] A. Teke, L. Saribulut, and M. Tümay, "A novel reference signal generation method for power quality improvement of unified power quality conditioner," *IEEE Trans. Power Del.,* Vol. 26, No. 4, pp. 2205-2214, Oct. 2011.

[14] V. Khadkikar, "Enhancing electric power quality using upqc: a comprehensive overview," *IEEE Trans. Power Electron.* Vol. 27, No. 5, pp.2284 - 2297, May 2012.

[15] D. Zmood and D. Holmes, "Stationary frame current regulation of PWM inverters with zero steady-state error," *IEEE Trans. Power Electron.*, Vol. 18, No. 3, pp. 814-822, May 2003.

[16] V. T. Phan, H. H. Lee, and T. W. Chun, "An improved control strategy using PI-resonant controller for unbalanced stand-alone doubly-fed induction generator," *J. Power Electron.*, Vol. 10, No. 2, pp. 194-202, Mar. 2010.

[17] M. P. Kazmierkowski, R. Krishnan, F. Blaabjerg, and J. D. Irwin, *Control in Power Electronics: Selected Problems*. San Diego, CA: Academic, 2002.

[18] R. Teodorescu, F. Blaabjerg, M. Liserre, and P. Loh, "Proportional-resonant controllers and filters for grid-connected voltage-source converters," in *Proc. IEE Electric. Power Appl.*, Vol. 153, No. 5, pp.750-762, Sep. 2006.

[19] *IEEE Recommended Practices and Requirements for Harmonic Control in Electrical Power Systems,* IEEE Standard 519-1992, 1992.

Quoc-Nam Trinh was born in Thanh-Hoa, Vietnam, in 1985. He received his B.S. in Electrical Engineering from the Ho Chi Minh City University of Technology, Ho Chi Minh City, Vietnam, in 2008. He is currently a combined M.S./Ph.D. student at the University of Ulsan, Ulsan, Korea. He is a member of the Korean Institute of Power Electronics (KIPE). His current research interests include Z-source inverters, wind power systems, active power filters, and power quality.

Hong-Hee Lee received his B.S., M.S., and Ph.D. in Electrical Engineering from Seoul National University, Seoul, Korea, in 1980, 1982, and 1990, respectively. He is currently a Professor in the School of Electrical Engineering, University of Ulsan, Ulsan, Korea. He is also the Director of the Network-based Research Center (NARC). His current research interests include power electronics, network-based motor control, and control networks. He is a member of the Institute of Electrical and Electronics Engineers (IEEE), the Korean Institute of Power Electronics (KIPE), the Korean Institute of Electrical Engineers (KIEE), and the Institute of Control, Automation, and Systems Engineers (ICASE).